JOURNAL OF CATALYSIS 93, 375–387 (1985)

Hydrodesulfurization Catalysis by Chevrel Phase Compounds

K. F. McCarty,*,† J. W. Anderegg,† and G. L. Schrader*,†,[1]

*Department of Chemical Engineering, and †Ames Laboratory–U.S. Department of Energy, Iowa State University, Ames, Iowa 50011

Received August 29, 1984; revised November 29, 1984

Reduced ternary molybdenum sulfides, known as Chevrel phase compounds, were investigated to determine their catalytic activity at 400°C for thiophene hydrodesulfurization and for 1-butene hydrogenation. Chevrel phase compounds of the general composition $M_xMo_6S_8$, with M being Ho, Pb, Sn, Ag, In, Cu, Fe, Ni, or Co, were found to have hydrodesulfurization activities comparable to model unpromoted and cobalt-promoted MoS_2 catalysts. The most active catalysts were the "large" cation compounds (Ho, Pb, Sn), and the least active catalysts were the "small" cation compounds (Cu, Fe, Ni, Co). Except for the nickel phase $Ni_{1.6}Mo_6S_8$, all Chevrel phase catalysts had hydrogenation activities which were much lower than the model MoS_2 catalysts. Fresh and used catalysts were characterized by X-ray diffraction, laser Raman spectroscopy, and X-ray photoelectron spectroscopy. While the bulk structures were stable under hydrodesulfurization reaction conditions, differences were observed in the stability of the surface molybdenum oxidation state for the specific classes of Chevrel phase catalysts: the oxidation state of the surface molybdenum atoms of the large cation compounds was found to be unchanged after 10 h of thiophene reaction, but some oxidation was apparent for the small cation compounds. The differences in stability can be related to the mobilities of the ternary metal atoms within the Chevrel phase structures.

INTRODUCTION

Catalytic hydrodesulfurization is most typically performed using catalysts which initially consist of molybdenum (Mo^{6+}) oxides dispersed on an alumina support (*1*). Catalytic activity is enhanced by addition of promoter elements, such as cobalt or nickel (*2, 3*). The presence of a MoS_2 (Mo^{4+}) phase in the reduced and sulfided catalysts has been established by a variety of techniques, such as X-ray diffraction (*4*), laser Raman spectroscopy (*5*), EXAFS (*6*), and X-ray photoelectron spectroscopy (*7*). A catalytically active Co–Mo–S (or Ni–Mo–S) phase has also been identified for supported $Co(Ni)Mo/Al_2O_3$ catalysts (*8*) and unsupported MoS_2 catalysts. This phase is thought to consist of cobalt (or nickel) atoms situated at the edges of MoS_2 crystallites (*9*). However, the complexity of the typical industrial supported $Co(Ni)Mo/Al_2O_3$ materials and even unsupported MoS_2-based catalysts has made characterization of the catalytically important material difficult. In addition, the extent to which the molybdenum chemistry can be altered is limited because of the predominance of MoS_2 for these catalysts.

This paper presents the results from an extended investigation (*10*) of a new class of hydrodesulfurization catalysts—reduced molybdenum sulfides known as Chevrel phase compounds.

Chevrel phase compounds are ternary molybdenum chalcogenides having a general formula $M_xMo_6Z_8$, with Z being sulfur, selenium, or tellurium and with M being a metallic ternary component (*11, 12*). These materials have been found to be active for thiophene desulfurization at 400°C under steady-state conditions. Their hydrogenation activity for 1-butene is relatively low, however, compared to conventional cobalt

[1] To whom correspondence should be addressed.

0021-9517/85 $3.00

molybdate catalysts. The discovery of the activity and selectivity of the Chevrel phases provides an important opportunity for systematically investigating the effect of variations in the molybdenum chemistry on the catalytic properties. Specifically, the importance of structure, the effect of various promoters, and the role of reduced (less than +4) molybdenum oxidation states can be examined.

Chevrel phase catalysts are structurally very different from conventional MoS_2-based catalysts. The anisotropic layer structure of MoS_2 involves trigonal prismatic coordination of the molybdenum atoms by six sulfur atoms; bonding is strong within layers, while only weak interactions exist between the layers. In contrast, the Chevrel phases exhibit a much different molybdenum structural chemistry. As metal-rich materials, the Chevrel phases are pseudomolecular compounds based on a Mo_6S_8 cluster. These Mo_6S_8 units exist as distorted molybdenum octahedra having apexes which lie slightly outside the face centers of a distorted cube of sulfur atoms; the Mo_6S_8 clusters are interconnected by Mo–S and Mo–Mo bonds.

Chevrel phase compounds also offer a significant opportunity for examining the promotional chemistry associated with molybdenum hydrodesulfurization catalysis. Nearly 40 metals can function as the ternary component for the Chevrel phases. The MoS_2 layer structure only permits intercalation of some alkali and alkaline earth elements (*13*). The location of catalytically important transition metals such as cobalt and nickel in catalysts based on MoS_2 is still uncertain. For the Chevrel phases, the location of the ternary metal "promoter" is much less ambiguous: the arrangement of Mo_6S_8 clusters in the lattice gives rise to infinite channels running parallel to the rhombohedral axis, and the ternary component atoms are located at specific crystallographic sites in these channels. The structure allows the accommodation of ternary component cations of "large" size (e.g., Ho, Pb, and Sn), "intermediate" size (e.g., Ag and In), and "small" size (e.g., Cu, Fe, Ni, Co). This classification of the Chevrel phases is based on the structural properties of the materials. The most important factors are the rhombohedral unit cell angle and the delocalization of the ternary component atoms (*11, 12*).

One of the most important aspects of molybdenum chemistry which can be investigated by using Chevrel phase catalysts is the molybdenum oxidation state. For conventional hydrodesulfurization catalysts, the dominant oxidation state is +4 due to the presence of MoS_2. In contrast, the Chevrel phase materials have formal oxidation states between +2 and $+2\frac{2}{3}$, depending on the concentration and/or valence of the ternary component.

EXPERIMENTAL METHODS

a. Catalyst Preparation

The Chevrel phase catalysts were prepared from mixtures of: $Mo_{2.06}S_3$; powdered molybdenum metal which was reduced at 1000°C in hydrogen for 18 h; and sulfides of the ternary component which were made by direct combination of the elements in evacuated, fused-silica tubes. The powders were thoroughly ground together, pressed into pellets, and heated in sealed, fused-silica tubes for 24 to 48 h at temperatures between 1000 and 1200°C before quenching in air (*14*). The $PbMo_6S_8$, $SnMo_6S_8$, $AgMo_6S_8$, and $InMo_6S_8$ materials were then ground in air, pressed into pellets, and reheated at temperatures between 1100 and 1200°C for 12 h. After the final heating, all synthesis tubes were opened in a nitrogen dry box, and the Chevrel phase pellets were lightly crushed. The 40–100 mesh portion was separated for use in activity measurements.

For the $PbMo_6S_8$, $SnMo_6S_8$, $AgMo_6S_8$, and $InMo_6S_8$ materials, all manipulations of the catalysts were performed in the dry box; other materials were stored in a dessicator in air for several days before the activity measurements were performed.

All compositions given are nominal except for the holmium, lead, tin, silver, and indium compounds which were prepared at compositions of $Ho_{1.2}Mo_6S_8$, $PbMo_{6.2}S_8$, $SnMo_{6.2}S_8$, $AgMo_{6.2}S_8$, and $InMo_{6.2}S_8$. Even though single crystal structure refinements have indicated that the ideal $M_{1.0}Mo_6S_8$ stoichiometry exists for the large cation compounds, it is often necessary to adjust the stoichiometry to obtain homogeneous, pure polycrystalline materials (*15*).

Representative unpromoted and cobalt-promoted MoS_2 catalysts were also prepared. Ammonium thiomolybdate was decomposed at 1000°C in a stream of helium, resulting in an unpromoted MoS_2 catalyst referred to as 1000°C MoS_2 (*16*). A cobalt-promoted MoS_2 catalyst was synthesized by the homogeneous precipitation technique of Candia *et al.* (*17*). Prepared with an atomic cobalt-to-molybdenum ratio of 1 to 4, the resulting material (referred to as $Co_{0.25}$–Mo_1–S) was pretreated at 450°C in a 2% H_2S–H_2 mixture for 4 h.

b. Activity Measurements

The activity measurements were performed in a $\frac{1}{4}$-in.-diameter stainless-steel reactor which could be operated in either the pulsed- or continuous-flow mode. Product separation and analysis was performed using a *n*-octane/Porasil C column and an Antek Model 310 gas chromatograph with a flame ionization detector. *trans*-2-Butene and 1,3-butadiene had identical retention times and were lumped together in the data analysis. Peak areas were measured by a Hewlett–Packard 3390A integrator.

High-purity helium (99.997%) and hydrogen (99.997%) were further purified by passage through copper traps for removal of oxygen and by passage through 4-Å molecular sieve traps for drying. Thiophene (Alfa Products, 99%) was subjected to several freeze–thaw cycles and was then dried over a 4-Å molecular sieve. Matheson 1-butene (99.5% CP) was dried using a 3-Å molecular sieve trap.

Hydrodesulfurization activities were measured at atmospheric pressure using thiophene as a model organo-sulfur compound. The amount of catalyst was adjusted to give a conversion of about 3% after 20 min of continuous thiophene flow. The reactor was filled with fresh catalyst and was then heated from room temperature to 400°C in a flow of helium at 19 ml/min (STP). The catalyst loadings for the reactor ranged from 0.0074 g for $Co_{0.25}$–Mo_1–S to 1.7875 g for $Cu_{3.2}Mo_6S_8$. After about 45 min, between ten and twenty-five 0.25-ml pulses of 2 mol% thiophene in hydrogen were injected into the reactor at 30-min intervals. The helium flow was then replaced by a continuous flow of 2 mol% thiophene in hydrogen at 22 ml/min (STP). After 10 h of reaction, the reactor was purged and cooled in a helium stream.

Hydrogenation activity measurements were performed in a pulsed-flow mode to minimize potential removal of sulfur from the Chevrel phase catalysts by hydrogen at 400°C. The reactor was filled with the same amount of fresh catalyst as in the hydrodesulfurization activity measurements. The reactor contents were heated from room temperature to 400°C in a stream of helium at 19 ml/min (STP) and held at 400°C for about 45 min. Two 0.10-ml pulses of 2 mol% 1-butene in hydrogen were injected into the reactor at a time spacing of 15 min. Twenty-five 0.10-ml pulses of 2% thiophene in hydrogen were then injected into the reactor, and the 1-butene pulses were repeated. After a continuous flow of thiophene in hydrogen for 2 h at 22 ml/min, the reactor was purged with helium, and the 1-butene pulses were repeated.

c. Catalyst Characterization

The initial surface areas of the catalysts and the surface area after 10 h of thiophene reaction were determined by the BET method using a Micromeritics 2100E Accu-Sorb instrument with krypton as the adsorbate. Krypton adsorption was used because of its accuracy in obtaining low surface area measurements (*18*).

X-Ray powder diffraction patterns were obtained with a Siemans D500 diffractometer using Cu$K\alpha$ radiation.

X-Ray photoelectron spectra (XPS) were obtained with an AEI 200B spectrometer using Al$K\alpha$ radiation. Samples were mounted on a double-sided adhesive tape, and all binding energies are referenced to a carbon 1*s* binding energy of 284.6 eV. Signal averaging was performed using a Nicolet 1180 computer system. In order to avoid air contamination, both the catalyst preparation tubes and the reactor were opened in a nitrogen dry box; portions of the samples were sealed in Pyrex tubes which were then opened in a helium dry box attached directly to the spectrometer. Spectra of the unused catalysts were obtained either from the powder of a freshly ground chunk of sample or from a 40–100 mesh portion of material with no further grinding (for the Pb Mo_6S_8, $SnMo_6S_8$, $AgMo_6S_8$, and $InMo_6S_8$ materials). Spectra of the used catalysts were obtained from the 40–100 mesh reactor charge with no further grinding. Raw peak areas were digitally integrated with no attempt made to correct for instrumental or atomic sensitivity factors. Also, no attempt was made to remove the area due to the sulfur 2*s* peak from the lower binding energy side of the molybdenum 3*d* doublet.

Laser Raman spectra were obtained using a Spex 1403 monochromator. The 514.5-nm line of a Spectra Physics 164 argon ion laser was operated at 200 mW (as measured at the source). Data was collected using backscattering geometry with spinning catalyst pellets. A Nicolet 1180E computer data acquisition system was used to accumulate 50 scans at a scanning speed of 2 cm^{-1}/s with 5 cm^{-1} resolution.

RESULTS

a. Activity Measurements

The continuous-flow thiophene reaction results for the Chevrel phase compounds and for the model MoS_2 materials are summarized in Table 1. The activities reported reflect a more accurate determination of the flame ionization detector relative response factors (*10, 19*). The hydrodesulfurization activities—that is, the rate of desulfurization normalized for surface area—were determined after 20 min and after 10 h of reaction. For the majority of catalysts, the surface areas after 10 h of reaction were within 10% of the surface areas for the fresh catalysts. For these materials, the activities were normalized on the basis of the initial surface areas. However, the surface areas of $Cu_{3.2}Mo_6S_8$, $Cu_{3.8}Mo_6S_8$, and $Fe_{1.5}Mo_6S_8$ increased considerably under reaction conditions; therefore the hydrodesulfurization activities of these materials after 10 h of reaction were normalized using the final surface areas.

The activities of the Chevrel phase catalysts are comparable to the activities of the model MoS_2 compounds. Indeed, after 10 h of reaction all large cation materials show higher activities than the model MoS_2 catalysts. It is very interesting that the activities of the Chevrel phase compounds can be grouped according to their structural classification, with the large cation compounds being the most active, the intermediate cation compounds being less active, and the small cation compounds being the least active. After 10 h of thiophene reaction, the order of activity is $HoMo_6S_8 > PbMo_6S_8 > SnMo_6S_8 > AgMo_6S_8 > InMo_6S_8 > Cu_xMo_6S_8 > Ni_{1.6}Mo_6S_8 > Fe_{1.5}Mo_6S_8 \approx Co_xMo_6S_8$. The most active Chevrel phase catalysts involve the unusual "promoters" Ho, Pb, and Sn; in contrast, the Chevrel phase compounds incorporating Ni and Co—the two most common conventional hydrodesulfurization promoters—are among the least active catalysts.

Table 1 also provides the hydrodesulfurization activities of a series of cobalt Chevrel catalysts, $Co_xMo_6S_8$, where x varies between 1.5 and 1.9. After 20 min of reaction, the activity increases in a roughly linear manner with increasing cobalt concentration. However, these differences in activity have decreased significantly after 10 h of reaction.

TABLE 1

Thiophene Hydrodesulfurization Activities (400°C)

Catalyst	Surface area (m^2/g)	Reaction time	Thiophene conversion (%)	HDS rate (mol/s · m^2) × 10^8	C_4 product distribution (%)			
					n-Butane	1-Butene	*trans*-2-Butene	*cis*-2-Butene
Large cation compounds								
$HoMo_6S_8$	0.579 ± 0.012[a]	20 min	2.48	12.65	0.9	32.2	41.2	25.7
		10 h	2.20	11.23	0.4	40.5	34.6	24.5
$PbMo_6S_8$	0.400 ± 0.007	20 min	1.92	10.03	1.0	54.4	26.0	18.5
		10 h	1.28	6.68	1.0	62.0	23.8	13.2
$SnMo_6S_8$	0.388 ± 0.002	20 min	1.90	3.57	0.6	60.7	22.6	16.1
		10 h	1.72	3.24	0.5	63.1	21.3	15.1
Intermediate cation compounds								
$AgMo_6S_8$	0.438 ± 0.004	20 min	2.59	5.12	1.1	36.5	39.1	23.3
		10 h	1.19	2.34	0.8	44.1	37.7	17.4
$InMo_6S_8$	0.625 ± 0.010	20 min	2.76	6.47	0.6	38.8	36.3	24.3
		10 h	0.89	2.08	—[b]	38.5	43.4	18.1
Small cation compounds								
$Cu_{3.2}Mo_6S_8$	0.090 ± 0.002	20 min	3.08	5.83	1.3	57.2	26.5	15.0
	0.180[c]	10 h[d]	1.95	1.84	0.6	58.9	28.6	11.9
$Cu_{3.8}Mo_6S_8$	0.081 ± 0.000	20 min	2.26	4.84	1.0	59.8	28.7	10.5
	0.099 ± 0.000	10 h[d]	1.04	1.82	1.3	56.9	33.5	8.3
$Fe_{1.5}Mo_6S_8$	0.093 ± 0.001	20 min	2.21	4.36	0.5	59.3	26.4	13.8
	0.131 ± 0.002	10 h[d]	0.79	1.10	—	57.2	33.8	9.0
$Ni_{1.6}Mo_6S_8$	0.144[e]	20 min	2.00	4.22	0.9	35.4	40.1	23.6
		10 h	0.71	1.50	—	35.0	46.4	18.6
$Co_{1.5}Mo_6S_8$	0.150 ± 0.004	20 min	2.06	3.16	0.4	46.4	34.2	19.0
		10 h	0.54	0.82	—	42.2	45.6	12.2
$Co_{1.6}Mo_6S_8$	0.099 ± 0.000	20 min	1.88	4.12	—	48.0	33.2	18.8
		10 h	0.47	1.02	—	44.8	44.6	10.6
$Co_{1.7}Mo_6S_8$	0.110 ± 0.000	20 min	2.05	3.65	—	46.1	35.5	18.4
		10 h	0.59	1.05	—	42.5	45.3	12.2
$Co_{1.8}Mo_6S_8$	0.080 ± 0.000	20 min	2.49	5.77	—	44.4	37.2	18.4
		10 h	0.52	1.20	—	40.1	48.5	11.4
$Co_{1.9}Mo_6S_8$	0.079 ± 0.002	20 min	2.11	4.70	0.4	47.6	35.3	16.7
	0.075[f]	10 h	0.51	1.13	—	42.9	46.5	10.6
Model MoS_2 compounds								
$Co_{0.25}$–Mo_1–S	10.83 ± 0.08	20 min	1.94	7.37	1.3	35.9	38.0	24.8
		10 h	0.77	2.92	1.5	36.4	41.1	21.0
1000°C MoS_2	3.40 ± 0.04	20 min	2.22	2.67	2.4	41.2	32.7	23.7
		10 h	0.76	0.92	1.8	46.0	34.9	17.3

[a] Errors estimated (95% confidence level) from least-squares fitting of adsorption data.
[b] Below detection limit.
[c] Average of two measurements: 0.180 ± 0.002, 0.180 ± 0.003 m^2/g.
[d] Results based on surface area after reaction.
[e] Average of two measurements: 0.137 ± 0.002, 0.150 ± 0.002 m^2/g.
[f] Average of two measurements: 0.074 ± 0.002, 0.076 ± 0.004 m^2/g.

The distribution of C_4 hydrocarbon products resulting from the desulfurization of thiophene varies considerably for the catalysts. For example, the ratio of the 2-butenes to 1-butene after 2 h of reaction is 2.1 for $HoMo_6S_8$, 0.78 for $PbMo_6S_8$, 0.66 for $SnMo_6S_8$, 1.3 for $AgMo_6S_8$, 1.6 for $InMo_6S_8$, 0.73 for $Cu_{3.2}Mo_6S_8$, 0.64 for $Fe_{1.5}Mo_6S_8$, 1.7 for $Ni_{1.6}Mo_6S_8$, 1.3 for $Co_{1.8}Mo_6S_8$, 1.1 for 1000°C MoS_2, and 1.7 for $Co_{0.25}$–Mo_1–S. This ratio reveals a deviation of the butene concentration from the thermodynamic equilibrium value at 400°C for which the ratio of 2-butenes to 1-butene is 2.8 (*20*).

Hydrogenation activities were calculated as the rate of production of *n*-butane from 1-butene and were normalized on the basis of the initial surface areas of the catalysts. The empty reactor produced 0.03% *n*-butane from 1-butene, and this value was subtracted from the *n*-butane yields before the activities were calculated. Data are pre-

TABLE 2

1-Butene Hydrogenation Activities (400°C)

Catalyst		HYD rate (mol/s · m²) × 10⁸	C_4 product distribution (%)			
			n-Butane	1-Butene	*trans*-2-Butene	*cis*-2-Butene
Large cation compounds						
$HoMo_6S_8$	A	0.3	0.06	90.5	4.6	4.8
	B	0.2	0.05	93.3	3.2	3.4
	C	0.3	0.06	31.2	38.6	30.1
$PbMo_6S_8$	A	0.2	0.03	76.2	11.8	11.9
	B	0.2	0.03	76.5	11.6	11.8
	C	0.2	0.03	68.1	15.7	16.1
$SnMo_6S_8$	A	0.1	0.05	47.0	27.9	25.0
	B	0.1	0.04	39.3	32.5	28.1
	C	0.1	0.06	46.6	27.8	25.5
Intermediate cation compounds						
$AgMo_6S_8$	A	0.1	0.08	26.0	41.8	32.1
	B	0.17	0.10	27.8	40.5	31.6
	C	0.40	0.23	26.5	41.8	31.4
$InMo_6S_8$	A	0.33	0.18	28.8	39.7	31.3
	B	0.33	0.18	25.7	42.2	31.9
	C	0.2	0.08	28.9	40.1	30.9
Small cation compounds						
$Cu_{3.2}Mo_6S_8$	A	0.1	0.07	41.5	31.4	27.0
	B	0.44	0.25	49.2	25.8	24.7
	C	0.30	0.17	51.2	23.9	24.7
$Cu_{3.8}Mo_6S_8$	A	0.20	0.10	53.8	23.2	22.9
	B	0.37	0.19	51.8	24.1	23.9
	C	0.1	0.07	80.0	9.5	10.4
$Fe_{1.5}Mo_6S_8$	A	0.1	0.05	91.7	4.2	4.0
	B	0.1	0.04	82.2	8.6	9.1
	C	0.1	0.04	78.8	10.1	11.0
$Ni_{1.6}Mo_6S_8$	A	0.27	0.14	22.8	46.9	30.1
	B	0.96	0.50	23.7	44.4	31.4
	C	0.68	0.36	26.9	41.5	31.2
$Co_{1.7}Mo_6S_8$	A	0.1	0.06	47.4	26.4	26.1
	B	0.2	0.09	40.9	29.5	29.5
	C	0.1	0.06	46.1	29.7	24.1
Model MoS_2 compounds						
$Co_{0.25}$–Mo_1–S	A	2.6	0.76	32.7	38.0	28.5
	B	1.1	0.33	39.2	33.9	26.5
	C	0.71	0.21	45.6	30.0	24.2
1000°C MoS_2	A	2.3	2.05	23.6	42.9	31.4
	B	2.4	2.08	23.9	42.6	31.4
	C	0.75	0.66	44.0	30.0	25.3
Calculated butene equilibrium at 400°C[a]				26.5	43.5	30.0

Note. A, fresh catalyst; B, after H_2–thiophene pulses; C, after 2 h continuous H_2–thiophene reaction.
[a] See Ref. (*20*).

sented in Table 2. Hydrogenation activities were measured in the pulsed mode in order to minimize the potential removal of sulfur from the catalysts by the sulfur-free hydrogenation feed. The activities were measured at three different times: (A) fresh, (B) after 25 pulses of thiophene-hydrogen, and (C) after 2 h of continuous-flow thiophene reaction. Except for the B and C measurements for $Ni_{1.6}Mo_6S_8$, the hydrogenation activities of the Chevrel phase catalysts are much lower than the model MoS_2 catalysts. The hydrogenation activities of all fresh Chevrel phase catalysts are between 7 and 30 times lower than the fresh model MoS_2 catalysts. Excluding $Ni_{1.6}Mo_6S_8$, the hydrogenation activities of the Chevrel phase catalysts after 2 h of thiophene reaction are still about 2 to 10 times lower than the model MoS_2 catalysts.

The catalysts also show a wide variation in their ability to isomerize the 1-butene–

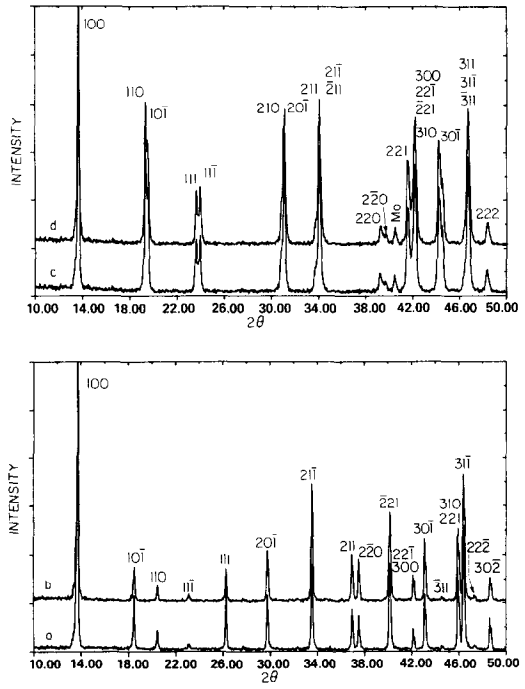

FIG. 1. X-Ray powder diffraction patterns of fresh and used (10-h thiophene reaction) Chevrel phase catalysts with rhombohedral *hkl* indexes: (a) fresh $Co_{1.7}Mo_6S_8$, (b) used $Co_{1.7}Mo_6S_8$, (c) fresh $HoMo_6S_8$, (d) used $HoMo_6S_8$.

hydrogen pulses to a mixture of 1-butene, *cis*-2-butene, and *trans*-2-butene. For example, after 2 h of thiophene reaction, 80% of the 1-butene pulse is unconverted by $Cu_{3.8}Mo_6S_8$; in contrast, only 26% of the 1-butene for the $AgMo_6S_8$ catalyst remains nonisomerized.

b. Catalyst Characterization

Figure 1 shows the X-ray powder diffraction patterns of two representative samples, $Co_{1.7}Mo_6S_8$ and $HoMo_6S_8$, before and after 10 h of thiophene reaction. As for all the Chevrel phase compounds studied, there are no apparent changes in the X-ray patterns after reaction.

The XPS binding energies of the catalysts are provided in Table 2, while Fig. 2 illustrates the molybdenum 3*d* doublets for the Chevrel phase catalysts in their fresh state and after 10 h of thiophene reaction. For the fresh catalysts, the Mo $3d_{5/2}$ binding energies are all grouped around 227.7 eV with $SnMo_6S_8$ being slightly higher (228.1 eV), $Ni_{1.6}Mo_6S_8$ and $Co_{1.7}Mo_6S_8$ being slightly lower (227.3 eV), and $AgMo_6S_8$ being considerably lower (226.6 eV). These results confirm the anticipated low molybdenum oxidation state. For comparison, the $3d_{5/2}$ binding energy of the Mo^{4+} in MoS_2 is about 228.9 eV (*21*). The XPS spectra obtained for several fresh Chevrel phase catalysts which had been stored in air for several months showed very minimal—but detect-

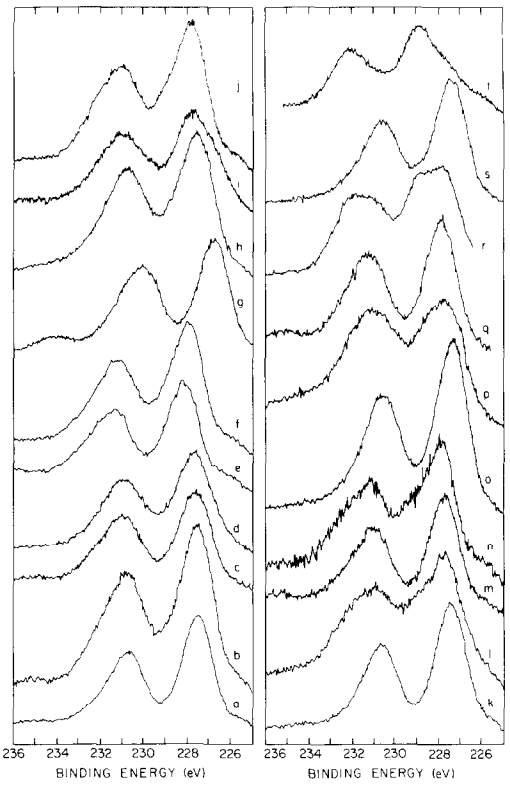

FIG. 2. Molybdenum 3*d* XPS spectra of fresh and used (10-h thiophene reaction) Chevrel phase catalysts: (a) fresh $HoMo_6S_8$, (b) used $HoMo_6S_8$, (c) fresh $PbMo_6S_8$, (d) used $PbMo_6S_8$, (e) fresh $SnMo_6S_8$, (f) used $SnMo_6S_8$, (g) fresh $AgMo_6S_8$, (h) used $AgMo_6S_8$, (i) fresh $InMo_6S_8$, (j) used $InMo_6S_8$, (k) fresh $Cu_{3.2}Mo_6S_8$, (l) used $Cu_{3.2}Mo_6S_8$, (m) fresh $Fe_{1.5}Mo_6S_8$, (n) used $Fe_{1.5}Mo_6S_8$, (o) fresh $Ni_{1.6}Mo_6S_8$, (p) used $Ni_{1.6}Mo_6S_8$, (q) fresh $Co_{1.6}Mo_6S_8$, (r) used $Co_{1.6}Mo_6S_8$, (s) fresh $Co_{1.7}Mo_6S_8$, (t) used $Co_{1.7}Mo_6S_8$.

TABLE 3

XPS Binding Energies and Intensity Ratios

Catalyst		Binding energies (EV) Mo $3d_{3/2}$	Mo $3d_{5/2}$	M —	M —	S 2p	Mo/M[a]
Large cation compounds							
$HoMo_6S_8$	A	230.7	227.5	—[b]	—	161.6	—
	B	230.8	227.5	—	—	161.5	—
$PbMo_6S_8$	A	230.9	227.5	142.3[c,1]	137.5[c,2]	161.6	1.8[d]
	B	230.8	227.5	142.5	137.5	161.8	1.8
$SnMo_6S_8$	A	231.4	228.1	494.5[e,1]	486.0[e,2]	161.7	2.1[f]
	B	231.2	227.9	494.5	455.9	161.8	2.2
Intermediate cation compounds							
$AgMo_6S_8$	A	230.0	226.6	373.9[e,1]	367.8[e,2]	161.9	2.6[f]
	B	230.7	227.5	373.1	367.2	161.7	8.1
$InMo_6S_8$	A	230.9	227.7	451.8[e,1]	444.2[e,2]	161.5	1.3[f]
	B	230.9	227.7	451.8	444.3	161.7	3.8
Small cation compounds							
$Cu_{3.2}Mo_6S_8$	A	230.7	227.4	951.5[g,1]	—	161.8	4.6[h]
	B	230.9	227.7	951.6	—	161.9	8.4
$Fe_{1.5}Mo_6S_8$	A	230.8	227.6	—	710.1[g,2]	161.7	0.8[i]
	B	231.0	227.7	—	710.1	162.1	—[j]
$Ni_{1.6}Mo_6S_8$	A	230.5	227.3	—	852.5[g,2]	161.5	9.4[i]
	B	231.1	227.8	—	852.5	161.4	28
$Co_{1.6}Mo_6S_8$	A	231.2	227.8	796.2[g,1]	780.4[g,2]	161.9	—[j]
	B	231.8	228.8	796.2	780.4	161.9	—
		229.9	227.8				
$Co_{1.7}Mo_6S_8$	A	230.6	227.3	795.1[g,1]	779.4[g,2]	161.8	3.4[i]
	B	231.9	228.7	796.6	780.8	162.2	4.4

Note. A, fresh catalyst; B, after 10 h continuous H_2–thiophene reaction.

[a] Raw area ratio of Mo 3*d* electrons to ternary component *M* electrons.

[b] Ho spectrum too diffuse to detect.

[c] *M* $4f_{5/2}$ (*c,1*) and $4f_{7/2}$ (*c,2*).

[d] Raw area ratio of Mo 3*d* to *M* 4*f*.

[e] *M* $3d_{3/2}$ (*e,1*) and $3d_{5/2}$ (*e,2*).

[f] Raw area ratio of Mo 3*d* to *M* 3*d*.

[g] *M* $2p_{1/2}$ (*g,1*) and $2p_{3/2}$ (*g,2*).

[h] Raw area ratio of Mo 3*d* to *M* $2p_{1/2}$.

[i] Raw area ratio of Mo 3*d* to *M* $2p_{3/2}$.

[j] Information not available.

able—changes from the air-isolated materials. For this reason, the $PbMo_6S_8$, $SnMo_6S_8$, $AgMo_6S_8$, and $InMo_6S_8$ materials were handled exclusively in the nitrogen-atmosphere dry box. The preparation of the holmium Chevrel phase was also repeated with the resulting material being handled entirely in the absence of air, as were the other large and intermediate cation compounds. Excellent reproducibility in the activity measurements and in the characterization results was observed for the holmium phases regardless of the absence or presence of oxygen.

Figure 2 shows the changes in the Mo 3*d* spectra which occur after 10 h of thiophene reaction. For the large cation compounds $HoMo_6S_8$, $PbMo_6S_8$, and $SnMo_6S_8$, there

are no apparent changes in the band positions or shapes. For the intermediate cation compound $AgMo_6S_8$, the Mo $3d_{5/2}$ peak shifts from 226.6 to 227.5 eV after reaction. For the other intermediate cation compound, $InMo_6S_8$, careful examination reveals the formation of shoulders on the high binding energy sides of the doublet, indicating some degree of oxidation of the surface molybdenum atoms. After thiophene reaction, the small cation materials all clearly show some degree of formation of a higher molybdenum oxidation state or states. For $Cu_{3.2}Mo_6S_8$ and $Fe_{1.5}Mo_6S_8$, the low oxidation state still dominates after reaction. However, after thiophene reaction using $Co_{1.6}Mo_6S_8$, a higher oxidation state of molybdenum with a $3d_{5/2}$ binding energy of about 228.8 eV appears. The intensity of this band is approximately equal to that of the lower molybdenum oxidation state. For the $Co_{1.7}Mo_6S_8$ catalyst, this higher oxidation state is of greater intensity than the lower oxidation state after reaction. The situation is less straightforward for the used $Ni_{1.6}Mo_6S_8$ molybdenum spectrum; while the $3d_{5/2}$ peak maximum is still at the low oxidation state value of 227.8 eV, both peaks of the doublet have become broader with a corresponding reduction in the "depth" of the "valley" between the peaks.

Except for the $Co_{1.7}Mo_6S_8$ and $AgMo_6S_8$ samples, the binding energies of the ternary components change little after reaction. Similarly, for all catalysts, the sulfur $2p$ binding energy is unaffected by reaction (consistently around 161.7 eV).

Table 3 also provides the ratios (Mo/M) of the raw peak areas for the molybdenum $3d$ electrons compared to a core electron orbital level of the ternary metal M. These ratios are not intended to quantitatively reflect the surface compositions since they are uncorrected for either instrumental or atomic sensitivity factors. Instead, they are provided to indicate changes in the surface compositions which occur after reaction for a particular Chevrel phase compound. (The diffuse nature of the holmium XPS spectra has prevented measurement of holmium binding energies or intensities (*22*).) For the large cation materials $PbMo_6S_8$ and $SnMo_6S_8$, the ratio Mo/M is unchanged after reaction. However, for all intermediate and small cation compounds, the ratio is larger after reaction than before, indicating a loss of ternary component atoms from the surface under reaction conditions.

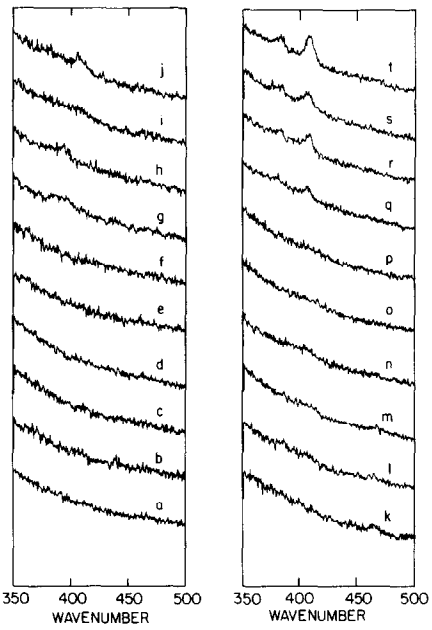

FIG. 3. Raman spectra of fresh and used (10-h thiophene reaction) Chevrel phase catalysts: (a) fresh $HoMo_6S_8$, (b) used $HoMo_6S_8$, (c) fresh $PbMo_6S_8$, (d) used $PbMo_6S_8$, (e) fresh $SnMo_6S_8$, (f) used $SnMo_6S_8$, (g) fresh $AgMo_6S_8$, (h) used $AgMo_6S_8$, (i) fresh $InMo_6S_8$, (j) used $InMo_6S_8$, (k) fresh $Cu_{3.2}Mo_6S_8$, (l) used $Cu_{3.2}Mo_6S_8$, (m) fresh $Fe_{1.5}Mo_6S_8$, (n) used $Fe_{1.5}Mo_6S_8$, (o) fresh $Ni_{1.6}Mo_6S_8$, (p) used $Ni_{1.6}Mo_6S_8$, (q) fresh $Co_{1.6}Mo_6S_8$, (r) used $Co_{1.6}Mo_6S_8$, (s) fresh $Co_{1.7}Mo_6S_8$, (t) used $Co_{1.7}Mo_6S_8$.

Figure 3 provides the Raman spectra of the fresh and used (10 h of thiophene reaction) Chevrel phase compounds in the region of the 383- and 409-cm^{-1} (*23*) bands of MoS_2. Raman spectroscopy is a very sensitive technique for the identification of both crystalline and poorly crystalline MoS_2 (*24*). A slight amount of MoS_2 impurity is indicated in the fresh $Co_{1.6}Mo_6S_8$ and $Co_{1.7}$

Mo_6S_8 catalysts, as was detected for the other cobalt Chevrel phase compounds. After reaction the amount of MoS_2 in these materials increased. The other fresh Chevrel phase catalysts show no presence of MoS_2. The origin of the weak 395-cm^{-1} band of $AgMo_6S_8$ is unexplained. Except for the used cobalt Chevrel phase compounds and the used $InMo_6S_8$, the Raman spectra of the used catalysts are devoid of MoS_2 features. The used $InMo_6S_8$ catalyst has a very weak 406-cm^{-1} band, which could possibly be due to MoS_2 impurities.

DISCUSSION OF RESULTS

The thiophene hydrodesulfurization activities of all Chevrel phase catalysts examined were comparable to those of the model unpromoted and cobalt-promoted MoS_2 catalysts (Table 1). Surface structure-based comparisons of activity with MoS_2 systems poses some challenges, however. The anisotropic structure of MoS_2 allows the existence of various ratios of the edge-to-basal-plane areas, and only very poor correlations between BET surface areas and hydrodesulfurization activities have been found (*25*). The normalization of activities by surface area in this study may bias the "intrinsic" kinetic parameters and somewhat alter the ordering of the catalysts according to activity; nevertheless, the high desulfurization activity of the Chevrel phase catalysts is clear.

For the Chevrel phase compounds which were examined in this study, the desulfurization activities are highest for the large cation compounds, followed by the intermediate cation compounds, with the small cation compounds being the least active. The cobalt and nickel Chevrel phase catalysts are among the least active catalysts studied, even though cobalt and nickel are the most widely used promoters in conventional hydrodesulfurization catalysts. It is the incorporation of the unusual "promoters" holmium, lead, and tin in the Chevrel phase structure which results in the most active catalysts.

X-Ray diffraction analysis and laser Raman spectroscopy have demonstrated the stability of the bulk structure of Chevrel phase compounds under reaction conditions. No loss of crystallinity or the formation of other phases was observed with X-ray diffraction. Except for the $Co_xMo_6S_8$ catalysts and possibly the used $InMo_6S_8$ catalyst, no crystalline or poorly crystalline MoS_2 impurities were observed either before or after reaction with laser Raman spectroscopy.

XPS analysis (Fig. 2) indicates that the stability of the reduced molybdenum oxidation states with respect to surface oxidation can be correlated with the structural properties of the Chevrel phase compounds. For the large cation compounds, molybdenum underwent no apparent oxidation under reaction conditions. For the intermediate cation compound $AgMo_6S_8$, an increase of nearly 1 eV in the Mo $3d_{5/2}$ binding energy after reaction indicated molybdenum oxidation. However, the final Mo $3d_{5/2}$ binding energy of 227.5 eV still represents a "reduced" molybdenum state which is comparable to the values found for the majority of fresh catalysts. A small degree of oxidation to Mo^{4+} was apparent for the other intermediate cation compound $InMo_6S_8$. Except for $Ni_{1.6}Mo_6S_8$, all small cation compounds clearly exhibited some formation of a Mo^{4+} state after reaction. This oxidation was greatest in the cobalt compounds $Co_xMo_6S_8$ for which the amount of MoS_2, as determined by Raman spectroscopy, was also found to increase after reaction. For $Ni_{1.6}Mo_6S_8$, the Mo $3d$ doublet was found to be broader after reaction, indicating the possible formation of a distribution of surface molybdenum oxidation states.

For the small and intermediate cation compounds, oxidation of the surface molybdenum was also accompanied by a loss of the ternary component from the surface (Table 3). However, the large cation compounds $PbMo_6S_8$ and $SnMo_6S_8$ exhibit no change in the ternary component concentration at the surface as a result of thio-

phene reaction. For the Chevrel phase materials, the presence of the ternary component is necessary for stability. For example, the binary compound Mo_6S_8 cannot be formed directly from the elements; rather it can be produced only by leaching out the ternary component from a small cation compound. While ternary Chevrel phases are stable at high temperature (*15*) (melting points of around 1700°C), Mo_6S_8 decomposes at about 400°C (*26*). Experiments performed in our research have revealed the formation of large amounts of MoS_2 (established by Raman spectroscopy) for Mo_6S_8 after thiophene reaction at times as short as 2 h and at temperatures as low as 300°C. Thus, the loss of the ternary component from the surface of the small and intermediate cation compounds can result in a material which is unstable toward partial oxidation.

The movement of the ternary metal is related to the potential "delocalization" of ternary atoms from their crystallographic positions in the Chevrel phase structure. For the small cation compounds, a high degree of delocalization (*27*) leads to large ionic conductivities even at low temperatures (*28*). For these materials, it is possible to electrochemically insert or remove the ternary component at room temperature (*29*). Under hydrodesulfurization conditions the ternary metal atoms can "retreat" into the bulk structure. The degree of delocalization is small for the large cation compounds (*27*). It is not possible to electrochemically insert or remove the ternary component for these structures (*30*). Recently (*31*), $PbMo_6S_8$ and $SnMo_6S_8$ have been successfully synthesized by thermally inserting lead and tin atoms into Mo_6S_8. Moderately high temperatures (470°C) and long reaction times (1 to 3 weeks) were required to overcome the low mobility of the ternary component atoms in the structure. This low mobility of the ternary metal for the large cation materials slows or prevents possible movement associated with the reactor conditions for hydrodesulfurization.

With the exception of $Ni_{1.6}Mo_6S_8$, the low hydrogenation activities of the Chevrel phase catalysts clearly distinguish them from the model MoS_2 catalysts (see Table 2). The combination of the high hydrodesulfurization activity and low hydrogenation activity of the Chevrel phase materials results in highly selective catalysts. For example, after 2 h of thiophene reaction, the ratio of hydrodesulfurization to hydrogenation is 50 for $HoMo_6S_8$, 66 for $PbMo_6S_8$, 35 for $SnMo_6S_8$, 8.5 for $AgMo_6S_8$, 23 for $InMo_6S_8$, 17 for $Cu_{3.2}Mo_6S_8$, 38 for $Fe_{1.5}Mo_6S_8$, 3.2 for $Ni_{1.6}Mo_6S_8$, and 17 for $Co_{1.7}Mo_6S_8$; in contrast, the values for the model catalysts are 7.5 for $Co_{0.25}$–Mo_1–S and 2.1 for 1000°C MoS_2. This selectivity may not be entirely unexpected since it is well known that for conventional Mo/Al_2O_3 catalysts the promotional effects of cobalt and nickel are much higher for hydrodesulfurization than for hydrogenation (*32*).

Hydrogenation and hydrodesulfurization are thought to occur at distinct sites on conventional $Co(Ni)Mo/Al_2O_3$ catalysts. Massoth *et al.* (*33*) have proposed that hydrodesulfurization occurs at vacancies on corner sites of MoS_2 while hydrogenation occurs at vacancies on edge sites. The isotropic nature of the Chevrel phase catalysts would, in contrast, provide only a few distinct types of geometrical sites, resulting in a high degree of catalytic selectivity. Alternatively, Candia *et al.* (*32*) have proposed that the two distinct sites of $Co(Ni)Mo/Al_2O_3$ catalysts are unpromoted molybdenum atoms and cobalt- or nickel-promoted molybdenum atoms. While the hydrogenation activity is thought to be about the same for either type of site, the promoted sites are thought to have much higher desulfurization activity; thus the latter activity is determined primarily by the concentration of these promoted sites. The uniform nature of the Chevrel phase compounds, with their direct incorporation of "promoter" atoms, should result in catalysts primarily with "promoted" molybdenum sites. The high desulfurization and low

hydrogenation activity of these "promoted" sites—and the concomitant lack of "unpromoted" sites—would be expected to result in high desulfurization rates and low hydrogenation rates. For $Ni_{1.6}Mo_6S_8$ following reaction, very little nickel was found at the catalyst surface (see Table 3). This lack of "promoter" atoms necessitated the formation of unpromoted sites, offering an explanation for the high hydrogenation activity of $Ni_{1.6}Mo_6S_8$.

These investigations using Chevrel phase compounds also have permitted the effect of reduced oxidation to be studied directly. The catalytic role of reduced molybdenum states less than Mo^{4+} has recently been addressed by other researchers also. For example, Konings *et al.* (*34*) correlated a Mo^{3+} ESR signal from supported molybdenum and tungsten catalysts with thiophene hydrodesulfurization activity. Valyon and Hall (*35*), after examining the chemisorption of O_2 and NO on reduced and sulfided Mo/Al_2O_3 catalysts, proposed that chemisorption occurs at the anion vacancy sites of adjacent Mo^{2+} atoms. Interestingly, O_2 chemisorption has been correlated with hydrodesulfurization activity for both unsupported MoS_2 catalysts (*25*) and Mo/Al_2O_3 catalysts (*36*). For conventional, sulfided hydrodesulfurization catalysts, the predominance of the Mo^{4+} state may obscure the presence of a catalytically important reduced molybdenum state (*35*). Furthermore, the degree to which the dominant molybdenum oxidation state may be altered in these materials is limited. The Chevrel phase catalysts, as confirmed with XPS analysis, allow direct synthesis of reduced molybdenum states. The hydrodesulfurization activity of these catalysts is high and comparable to model conventional catalysts. Most importantly, however, is that the hydrodesulfurization activity is highest for the most stable—and thus the most reduced—Chevrel phase compounds.

CONCLUSIONS

Chevrel phase compounds have been found to be useful model hydrodesulfurization catalysts which permit the effect of systematic variations in molybdenum chemistry on catalytic selectivity and activity to be investigated. The materials process high hydrodesulfurization activity which is dependent on the structural type of the compound. Large cation compounds with their unusual "promoter" elements are the most active, intermediate cation compounds are the next most active, and small cation compounds demonstrate the lowest activity. Hydrogenation activities are low except for the used $Ni_{1.6}Mo_6S_8$ catalyst. All bulk structures were stable under reaction conditions. For the small and intermediate cation compounds, some surface oxidation of molybdenum was observed. The surface oxidation is a result of the movement of the ternary metal component away from the surface and into the bulk. However, the reduced molybdenum oxidation states of the large cation compounds are stable under reaction conditions.

ACKNOWLEDGMENTS

This work was conducted through the Ames Laboratory which is operated for the U.S. Department of Energy by Iowa State University under Contract W-7405-Eng-82. This research was supported by the Office of Basic Energy Sciences, Chemical Sciences Division.

REFERENCES

1. Grange, P., *Catal. Rev.-Sci. Eng.* **21**(1), 135 (1980).
2. Wivel, C., Candia, R., Clausen, B. S., Mørup, S., and Topsøe, H., *J. Catal.* **68,** 453 (1981).
3. Bachelier, J., Duchet, J. C., and Cornet, D., *J. Catal.* **87,** 283 (1984).
4. Pollack, S. S., Makovsky, L. E., and Brown, F. R., *J. Catal.* **59,** 452 (1979).
5. Schrader, G. L., and Cheng, C. P., *J. Catal.* **80,** 369 (1983).
6. Parham, T. G., and Merrill, R. P., *J. Catal.* **85,** 295 (1984).
7. Li, C. P., and Hercules, D. M., *J. Phys. Chem.* **88,** 456 (1984).
8. Topsøe, H., Clausen, B. S., Candia, R., Wivel, C., and Mørup, S., *J. Catal.* **68,** 433 (1981).
9. Topsøe, N. Y., and Topsøe, H., *J. Catal.* **84,** 386 (1983).

10. McCarty, K. F., and Schrader, G. L., *Ind. Eng. Chem. Prod. Res. Dev.* **23,** 519 (1984).
11. Chevrel, R., and Sergent, M., *in* "Topics in Current Physics" (Ø. Fischer and M. B. Maple, Eds.), Vol. 34, p. 25. Springer, Berlin, 1982.
12. Yvon, K., *in* "Topics in Current Physics" (Ø. Fischer and M. B. Maple, Eds.), Vol. 34, p. 87. Springer, Berlin, 1982.
13. Schöllhorn, R., Kümpers, M., and Plorin, D., *J. Less-Common Met.* **58,** 55 (1978).
14. Lynn, J. W., Shirane, G., Thomlinson, W., Shelton, R. N., and Moncton, D. E., *Phys. Rev. B* **24**(7), 3817 (1981).
15. Flükiger, R., and Baillif, R., *in* "Topics in Current Physics" (Ø. Fischer and M. B. Maple, Eds.), Vol. 34, p. 113. Springer, Berlin, 1982.
16. Wildervanck, J. C., and Jellinek, F., *Z. Anorg. Chem.* **328,** 309 (1964).
17. Candia, R., Clausen, B. S., and Topsøe, H., *Bull. Soc. Chim. Belg.* **90**(12), 1225 (1981).
18. Gregg, S. J., and Sing, K. S. W., "Adsorption, Surface Area, and Porosity." Academic Press, New York, 1967.
19. McCarty, K. F., and Schrader, G. L., "Proceedings, 8th International Congress on Catalysis," Vol. 4, p. 427. Verlag Chemie, Weinheim, 1984.
20. Benson, S. W., and Bose, A. W., *J. Amer. Chem. Soc.* **85,** 1385 (1963).
21. Patterson, T. A., Carver, J. C., Leyden, D. E., and Hercules, D. M., *J. Phys. Chem.* **80**(15), 1700 (1976).
22. Lang, W. C., Padalia, B. D., Watson, L. M., Fabian, D. J., and Norris, P. R., *Faraday Discuss. Chem. Soc.* **60,** 37 (1975).
23. Weiting, T. J., and Verble, J. L., *Phys. Rev. B* **3**(12), 4286 (1971).
24. Chang, C. H., and Chan, S. S., *J. Catal.* **72,** 139 (1981).
25. Tauster, S. J., Pecoraro, T. A., and Chianelli, R. R., *J. Catal.* **63,** 515 (1980).
26. Cheung, K. Y., and Steele, B. C. H., *Solid State Ionics* **1,** 337 (1980).
27. Yvon, K., *in* "Current Topics in Materials Science" (E. Kaldis, Ed.), Vol. 3, p. 53. North-Holland, Amsterdam, 1979.
28. Dudley, G. J., Cheung, K. Y., and Steele, B. C. H., *J. Solid State Chem.* **32,** 259 (1980).
29. Schöllhorn, R., Kümpers, M., and Besenhard, J. O., *Mater. Res. Bull.* **12,** 781 (1977).
30. Umarji, A. M., Subba Rao, G. V., Janawadkar, M. P., and Radhakrishnan, T. S., *J. Phys. Chem. Solids* **41,** 421 (1980).
31. Tarascon, J. M., Disalvo, F. J., Murphy, D. W., Hull, G. W., Rietman, E. A., and Waszczak, J. V., *J. Solid State Chem.* **54,** 204 (1984).
32. Candia, R., Clausen, B. S., Bartholdy, J., Topsøe, N. Y., Lengeler, B., and Topsøe, H., "Proceedings, 8th International Congress on Catalysis," Vol. 2, p. 375. Verlag Chemie, Weinheim, 1984.
33. Massoth, F. E., Muralidhar, G., and Shabtai, J., *J. Catal.* **85,** 53 (1984).
34. Konings, A. J. A., Valster, A., de Beer, V. H. J., and Prins, R., *J. Catal.* **76,** 466 (1982).
35. Valyon, J., and Hall, W. K., *J. Catal.* **84,** 216 (1983).
36. Bachelier, J., Duchet, J. C., and Cornet, D., *Bull. Soc. Chim. Belg.* **90**(12), 1301 (1981).